Reconciling exchange striction with biquadratic exchange in $KMn_{0.1}Zn_{0.9}F_3$: An inelastic neutron scattering study

A. Furrer,[1] F. Juranyi,[1] K. W. Krämer,[2] and Th. Strässle[1]
[1]*Laboratory for Neutron Scattering, ETH Zurich and PSI Villigen, CH-5232 Villigen PSI, Switzerland*
[2]*Department of Chemistry and Biochemistry, University of Bern, CH-3012 Bern, Switzerland*
(Received 18 January 2008; revised manuscript received 5 March 2008; published 3 April 2008)

Non-negligible higher-order exchange terms are ubiquitous in the spin Hamiltonians of a large variety of magnetic compounds. Yet the origin of higher-order exchange has not been satisfactorily established. This question was addressed by performing inelastic neutron scattering experiments for the magnetically diluted compound $KMn_{0.1}Zn_{0.9}F_3$. The observed excitations can be associated with transitions between the low-lying electronic states of Mn^{2+} multimers which are well described by a spin Hamiltonian including bilinear and biquadratic exchange interactions. The bilinear exchange parameter J derived from the dimer spectra exhibits a strong temperature dependence, whereas the biquadratic exchange parameter K is independent of temperature. By minimizing the total elastic and magnetic energy of the dimer, we can express the parameter K in terms of lattice, elastic, and magnetic properties. The good agreement between the calculated and observed values of K indicates that the mechanism of exchange striction is the likely origin of the biquadratic interaction in the title compound.

DOI: 10.1103/PhysRevB.77.134410 PACS number(s): 71.70.Gm, 75.30.Et, 78.70.Nx

I. INTRODUCTION

The magnetic properties of localized S-state systems are usually interpreted in terms of the Heisenberg model which is based on the bilinear spin permutation operator,[1]

$$P_{ij} = \tfrac{1}{2}(1 + \mathbf{S_i} \cdot \mathbf{S_j}). \quad (1)$$

A more complete Hamiltonian takes permutations of more than two spins into account. The relevant terms up to second order (biquadratic terms) are defined by

$$P_{ij}^2 = \tfrac{1}{4}[1 + 2\mathbf{S_i} \cdot \mathbf{S_j} + (\mathbf{S_i} \cdot \mathbf{S_j})^2], \quad (2a)$$

$$P_{ij}P_{jk} = \tfrac{1}{4}[1 + \mathbf{S_i} \cdot \mathbf{S_j} + \mathbf{S_j} \cdot \mathbf{S_k} + (\mathbf{S_i} \cdot \mathbf{S_j})(\mathbf{S_j} \cdot \mathbf{S_k})], \quad (2b)$$

$$P_{ij}P_{kl} = \tfrac{1}{4}[1 + \mathbf{S_i} \cdot \mathbf{S_j} + \mathbf{S_k} \cdot \mathbf{S_l} + (\mathbf{S_i} \cdot \mathbf{S_j})(\mathbf{S_k} \cdot \mathbf{S_l})], \quad (2c)$$

which refer to two-spin, three-spin, and four-spin interactions, respectively. There is increasing evidence for the importance of higher-order and multispin interactions; the most prominent example being the cyclic exchange of type (2c) in the high-T_c parent compound La_2CuO_4 which contributes about 25% to the total exchange energy as determined by an analysis of the spin-wave dispersion.[2] Three-spin [type (2b)] interactions are relevant to model the excitation spectra of Mn^{2+} trimers in $CsMn_{0.28}Mg_{0.72}Br_3$.[3] There is ample evidence for the existence of biquadratic two-spin terms of type (2a) in both molecular magnetic compounds[4] and insulators doped with magnetic ions.[5,6]

The present work addresses the origin of the biquadratic two-spin term of type (2a). In principle, biquadratic exchange can arise as an intrinsic second-order exchange term in Anderson's theory of superexchange.[7] Anderson estimated the ratio K/J of biquadratic to bilinear exchange to be about 1%. Alternatively, Kittel suggested that an effective biquadratic term can occur as a result of exchange striction, which is based on a balance between elastic and magnetic exchange forces.[8] Early electron paramagnetic resonance (EPR) experiments performed for Mn^{2+} pairs in MgO and CaO gave evidence for a ratio $K/J \approx 5\%$, which could be explained to a large extent by exchange striction, but the additional presence of intrinsic higher-order exchange could not be ruled out.[5] A more recent study of Mn^{2+} pairs in $CsMgBr_3$ with $K/J \approx 0.5\%$ concluded that exchange striction is the major contribution to the biquadratic exchange; however, intrinsic higher-order exchange could not be completely excluded due to some approximations used for the calculation of the elastic properties.[6] An ideal candidate to discriminate between intrinsic higher-order exchange and exchange striction would be a compound with an extremely small ratio K/J. This condition is fulfilled, e.g., for the compound $KMn_xZn_{1-x}F_3$ with $K/J \approx 0.1\%$.

In this paper, we describe the results of an inelastic neutron scattering study of the spin-excitation spectra of isolated multimers of Mn^{2+} ions randomly substituted for 10% of the nonmagnetic Zn^{2+} ions in the $KZnF_3$ perovskite lattice. The experimental procedure is described in Sec. II, followed in Sec. III by a summary of the spin Hamiltonians, energy levels, neutron cross sections, and cluster probabilities for Mn^{2+} multimers. The observed energy spectra gave evidence for scattering from Mn^{2+} dimers up to Mn^{2+} pentamers as described in Sec. IV, which includes a detailed analysis of the Mn^{2+} dimer excitations. The magnetoelastic effects are worked out in Sec. V, which provides strong evidence that exchange striction can quantitatively account for the observed biquadratic exchange interaction in $KMn_{0.1}Zn_{0.9}F_3$.

II. EXPERIMENT

A sample of 10 g $KMn_{0.1}Zn_{0.9}F_3$ was prepared from stoichiometric amounts of KHF_2, ZnO, and $MnCO_3$. The salts were heated twice with 20 ml of concentrated aqueous HF acid in a teflon beaker and evaporated to dryness. The obtained powder was transferred into a glassy carbon crucible

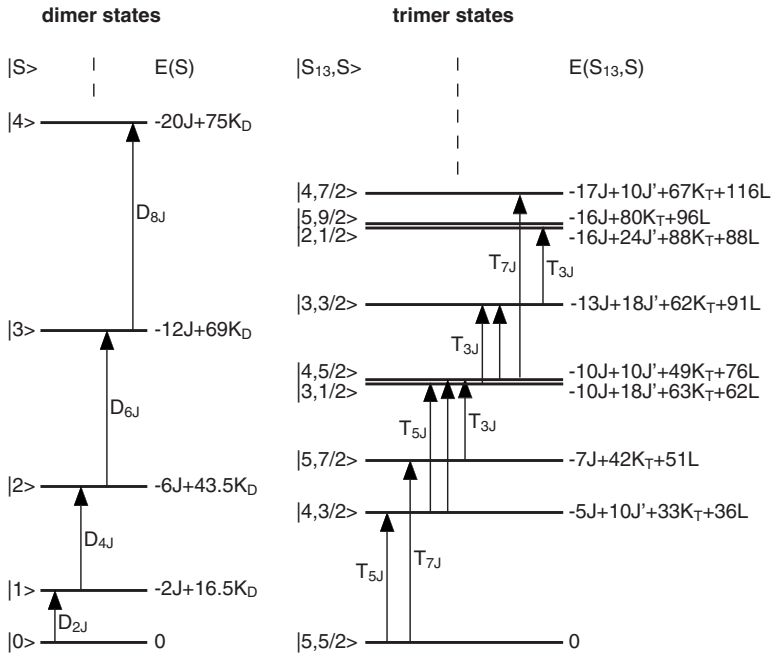

FIG. 1. Energy level splittings for dimers and trimers of Mn^{2+} ions. The transitions allowed by the selection rules [Eq. (8)] are indicated by arrows.

and fluorinated with an Ar/HF gas mixture at 600 °C for 20 h. Finally, the product was molten up at 920 °C for 8 h and crystallized by cooling to room temperature. The melt was sealed under vacuum in a welded platinum crucible. The purity of the light pink product was checked by powder x-ray diffraction. $KMn_{0.1}Zn_{0.9}F_3$ crystallizes in the perovskite structure, space group $Pm3m$, with a lattice parameter $a=4.0719(2)$ Å. This is in good agreement with a linear interpolation of the lattice parameter between the pure compounds $KZnF_3$ and $KMnF_3$ which are reported as $a=4.0611(9)$ Å (Ref. 9) and $a=4.186$ Å,[10] respectively.

The inelastic neutron scattering experiments were carried out with use of the high-resolution time-of-flight spectrometer FOCUS at the spallation neutron source SINQ at PSI Villigen. The measurements were performed with incoming neutron energies of 4.42 and 2.27 meV, giving energy resolutions at the elastic position of 0.181 and 0.047 meV, respectively. According to simulations (using the time-focusing principle), the energy resolutions are gradually improving with increasing energy transfer on the energy-loss side of the spectrum, typically by 25% at energy transfers corresponding to half the incoming neutron energy. The scattered neutrons were detected by an array of ^{3}He counters covering a large range of scattering angles $10° \leq \Phi \leq 130°$. The sample was enclosed in an Al cylinder (12 mm diameter, 45 mm height) and placed into a He cryostat. Energy spectra were taken at $T=1.5$, 20, 50, 100, 150, and 200 K. Additional experiments were performed for the empty container as well as for vanadium to allow the correction of the raw data with respect to background, detector efficiency, absorption, and detailed balance effects according to standard procedures.

III. THEORETICAL BACKGROUND

A. Spin Hamiltonian

For a dimer, the spin Hamiltonian, up to second order in the spin operators, can be written as

$$\mathcal{H}_D = -2J\mathbf{S}_1 \cdot \mathbf{S}_2 - K_D(\mathbf{S}_1 \cdot \mathbf{S}_2)^2, \tag{3}$$

where J and K_D are the bilinear and biquadratic exchange parameters, respectively. Equation (3) is diagonal in the basis $|S\rangle$, where S denotes the total dimer spin $\mathbf{S}=\mathbf{S}_1+\mathbf{S}_2$, with $0 \leq S \leq 2S_i$. The eigenvalues are given by

$$E(S) = -J\eta - \tfrac{1}{4}K_D\eta^2, \tag{4}$$

where $\eta=S(S+1)-2S_i(S_i+1)$. The energy level sequence as well as the energy eigenvalues $E(S)$ for Mn^{2+} ions ($S_i=\frac{5}{2}$) are shown in Fig. 1 for antiferromagnetic exchange $J<0$. For $K_D=0$, the energy splitting pattern satisfies the Landé interval rule $E(S)-E(S-1)=-2JS$.

For a trimer, the spin Hamiltonian is described by

$$\begin{aligned}\mathcal{H}_T = &-2[J(\mathbf{S}_1 \cdot \mathbf{S}_2 + \mathbf{S}_2 \cdot \mathbf{S}_3) + J'\mathbf{S}_1 \cdot \mathbf{S}_3] \\ &- K_T[(\mathbf{S}_1 \cdot \mathbf{S}_2)^2 + (\mathbf{S}_2 \cdot \mathbf{S}_3)^2] \\ &- L[(\mathbf{S}_1 \cdot \mathbf{S}_2)(\mathbf{S}_2 \cdot \mathbf{S}_3) + (\mathbf{S}_3 \cdot \mathbf{S}_2)(\mathbf{S}_2 \cdot \mathbf{S}_1)],\end{aligned} \tag{5}$$

where J' and L denote the bilinear next-nearest-neighbor and biquadratic three-spin exchange parameters, respectively. We use the coupling scheme $\mathbf{S}_{13}=\mathbf{S}_1+\mathbf{S}_3$ and $\mathbf{S}=\mathbf{S}_1+\mathbf{S}_2+\mathbf{S}_3$, with $0 \leq S_{13} \leq 2S_i$ and $|S_{13}-S_i| \leq S \leq |S_{13}+S_i|$, respectively. The trimer states are therefore defined by the wave functions $|S_{13},S\rangle$. For $K_T \neq 0$ and $L \neq 0$, Hamiltonian (5) is not diagonal. Figure 1 shows the resulting low-energy part of the split-

ting pattern as well as the energy eigenvalues $E(S_{13},S)$ for Mn^{2+} ions ($S_i=\frac{5}{2}$) and $J<0$.

For clusters with four and more magnetic ions, the diagonalization of the spin Hamiltonian progressively becomes cumbersome, but the total spin S remains a good quantum number. We refer to Fig. 2 of Ref. 11 for the low-energy parts of the splitting patterns of Mn^{2+} tetramers, pentamers, and hexamers.

EPR experiments performed for exchange-coupled pairs of Mn^{2+} ions in $KZnF_3$ (Ref. 12) gave evidence for the existence of a single-ion anisotropy term of the form

$$\mathcal{H}_{\rm an} = D\sum_i (S_i^Z)^2, \tag{6}$$

which we eventually have to add to spin Hamiltonians (3) and (5). The anisotropy term has the effect of splitting the spin states $|S\rangle$ into the states $|S,\pm M\rangle$ where the additional spin quantum number M is defined by $-S\leqslant M\leqslant S$.

B. Neutron cross section

For spin dimers and polycrystalline material, the neutron cross section for a transition from the initial state $|S\rangle$ to the final state $|S'\rangle$ is defined by[13]

$$\frac{d^2\sigma}{d\Omega d\omega} = 2C\left\{1+(-1)^{\Delta S}\frac{\sin(QR)}{QR}\right\}|\langle S'\|\hat{T}\|S\rangle|^2, \tag{7a}$$

which corresponds to the sum of the transitions $|S,M\rangle\Rightarrow|S',M'\rangle$ with $\Delta M=+1$, $\Delta M=0$, and $\Delta M=-1$

$$\left.\frac{d^2\sigma}{d\Omega d\omega}\right|_{\Delta M=0} = C\left\{\frac{2}{3}+(-1)^{\Delta S}\left[\frac{2\sin(QR)}{Q^3R^3}-\frac{2\cos(QR)}{Q^2R^2}\right]\times|\langle S'\|\hat{T}\|S\rangle|^2\right\}, \tag{7b}$$

$$\left.\frac{d^2\sigma}{d\Omega d\omega}\right|_{\Delta M=+1} = C\left\{\frac{2}{3}-(-1)^{\Delta S}\left[\frac{\sin(QR)}{Q^3R^3}-\frac{\cos(QR)}{Q^2R^2}-\frac{\sin(QR)}{QR}\right]|\langle S'\|\hat{T}\|S\rangle|^2\right\}, \tag{7c}$$

with

$$C = N\left(\frac{\gamma e^2}{m_e c^2}\right)^2\rho_{S,M}\frac{k'}{k}F^2(Q)\times\exp\{-2W(Q)\}\delta\{\hbar\omega+E(S,M)-E(S',M')\}. \tag{7d}$$

The cross section for $\Delta M=-1$ is identical to Eq. (7c). N is the total number of spin dimers in the sample, $\rho_{S,M}$ is the population of the initial state $|S,M\rangle$ governed by the Boltzmann statistics, k and k' are the wave numbers of the incoming and scattered neutrons, respectively, $\mathbf{Q}=\mathbf{k}-\mathbf{k}'$ is the scattering vector, $F(Q)$ is the magnetic form factor, $\exp\{-2W(Q)\}$ is the Debye–Waller factor, $\hbar\omega$ is the energy transfer, $E(S,M)$ and $E(S',M')$ are the energies of the initial and final states, respectively, R is the distance between the two spins, and $\langle S'\|\hat{T}\|S\rangle$ is the reduced transition matrix element defined in Ref. 14. The remaining symbols have their usual meaning. The transition matrix elements carry essential information to derive the selection rules for spin dimers,

$$\Delta S = S-S' = 0,\pm1, \quad \Delta M = M-M' = 0,\pm1. \tag{8}$$

Formulas for the neutron cross section of spin trimers and spin tetramers were given in Refs. 15 and 4, respectively. For spin trimers, the condition $\Delta S_{13}=0,\pm1$ has to be added to the selection rules [Eq. (8)]. The allowed transitions for Mn^{2+} dimers and trimers are indicated by arrows in Fig. 1. We realize that all excitation energies are integer multiples of J (for $J'=K_{\rm D}=K_{\rm T}=L=0$) which is convenient to identify the observed transitions.

C. Cluster probabilities

Isolated clusters of Mn^{2+} ions in $KMn_xZn_{1-x}F_3$ simply occur because of the random distribution of Mn^{2+} and Zn^{2+} ions over the sites of the cubic perovskite lattice. The cluster probabilities for monomers, dimers, and trimers are given by

$$p_{\rm M} = (1-x)^6, \quad p_{\rm D} = 6x(1-x)^{10}, \quad p_{\rm T} = 9x^2(1-x)^{14}+24x^2(1-x)^{13}, \tag{9}$$

respectively, where the first and second terms of $p_{\rm T}$ refer to trimers with bond angles of 180° and 90°, respectively. We chose the Mn^{2+} concentration $x=0.1$ in order to maximize the number of dimers as well as to be well below the percolation limit for the existence of long-range magnetic order, which is $x_p=0.312$ under the assumption that the Mn^{2+} ions essentially interact with nearest-neighbor exchange.[16] For $x=0.1$, we find $p_{\rm M}=0.531$, $p_{\rm D}=0.209$, and $p_{\rm T}=0.083$. We recognize that with increasing cluster size, the decrease in the cluster probabilities of a three-dimensional compound such as $KMn_xZn_{1-x}F_3$ is much less pronounced than for one-dimensional compounds such as $CsMn_xMg_{1-x}Br_3$,[6] so that the experimental data anticipated for dimers are likely to be contaminated by contributions from unwanted larger clusters.

IV. RESULTS AND DATA ANALYSIS

Energy spectra of neutrons scattered from $KMn_{0.1}Zn_{0.9}F_3$ at $T=20$ K and $T=100$ K are shown in Fig. 2. We can easily attribute the well-defined inelastic peaks to particular multimer transitions according to the energy splitting patterns of Fig. 1. The dimer transitions denoted by D_{2J}, D_{4J}, D_{6J}, and D_{8J} nicely satisfy the Landé interval rule predicted in Eq. (4) with coupling parameters $J\approx-0.4$ meV and $|K_{\rm D}|\ll|J|$. The peaks denoted by T_{3J}, T_{5J}, and T_{7J} can then be identified as trimer transitions. Furthermore, there is evidence for unresolved scattering at energies of approximately 5.5, 7.5, and 6.5 J which according to Fig. 2 of Ref. 11 can be attributed to tetramer ($Te_{5.5\ J}$ and $Te_{7.5\ J}$) and pentamer ($P_{6.5\ J}$) transitions, respectively. Phonon scattering can be excluded, since the lowest peak of the phonon density of states lies at about 8 meV (Ref. 17) which is far outside the considered energy range. A Gaussian least-squares fit was applied to the observed energy spectra to yield the positions and intensities of the peaks for a more detailed analysis. The linewidths of all the peaks were kept fixed slightly above the instrumental

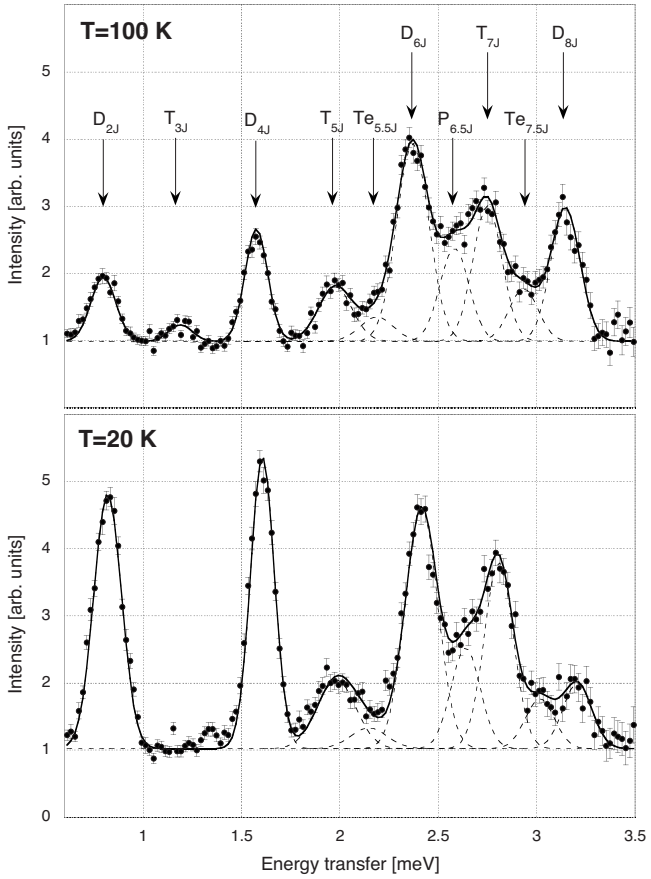

FIG. 2. Energy spectra of neutrons scattered from $KMn_{0.1}Zn_{0.9}F_3$ at $T=20$ and 100 K. The incoming neutron energy was 4.42 meV. The positions of the multimer transitions are indicated by arrows (D=dimer, T=trimer, Te=tetramer, P=pentamer). The lines are the results of a least-squares fitting procedure explained in the text.

energy resolution in order to account for level splittings due to the single-ion anisotropy as well as for overlap of ground-state and excited-state trimer transitions. The results for the dimer and trimer transitions are listed in Tables I and II, respectively.

With increasing temperature, the peak positions marginally move to lower energies. Furthermore, we observe a redistribution of the spectral weight of all the peaks in agreement with the Boltzmann population factor. The peak identification indicated in Fig. 2 was confirmed by detailed calculations of the T and Q dependences of the intensities according to the dimer and trimer neutron cross sections weighted by the corresponding cluster probabilities.

TABLE I. Temperature dependence of dimer excitation energies and model parameters (J, K_D) of $KMn_{0.1}Zn_{0.9}F_3$.

T (K)		D_{2J} (meV)	D_{4J} (meV)	D_{6J} (meV)	D_{8J} (meV)	J (meV)	K_D (μeV)
20	Obs.	0.817(2)	1.604(3)	2.408(4)	3.198(13)		
	Calc.	0.808	1.612	2.408	3.193	−0.3987(26)	0.63(51)
50	Obs.	0.812(2)	1.596(2)	2.396(3)	3.171(6)		
	Calc.	0.803	1.603	2.393	3.171	−0.3958(18)	0.72(38)
100	Obs.	0.802(3)	1.582(2)	2.379(3)	3.148(4)		
	Calc.	0.796	1.588	2.374	3.150	−0.3933(12)	0.54(29)
150	Obs.	0.796(3)	1.562(3)	2.338(5)	3.094(5)		
	Calc.	0.786	1.568	2.338	3.093	−0.3859(15)	0.89(33)
200	Obs.	0.779(6)	1.538(4)	2.303(4)	3.039(8)		
	Calc.	0.774	1.543	2.300	3.041	−0.3794(9)	0.93(22)

TABLE II. Temperature dependence of trimer excitation energies for $KMn_{0.1}Zn_{0.9}F_3$.

T (K)		T_{3J} (meV)	T_{5J} (meV)	T_{7J} (meV)	J (meV)	$K_T=L_T$ (μeV)
20	Obs.		2.000(8)	2.805(7)		
	Calc.	1.209(18)	2.021(35)	2.828(49)	−0.3987(26)	0.42(34)
50	Obs.	1.190(15)	1.990(8)	2.795(13)		
	Calc.	1.201(13)	2.009(25)	2.810(34)	−0.3958(18)	0.48(26)
100	Obs.	1.188(12)	1.973(8)	2.756(9)		
	Calc.	1.190(10)	1.989(18)	2.781(24)	−0.3933(12)	0.36(20)
150	Obs.	1.172(8)	1.968(7)	2.716(6)		
	Calc.	1.175(11)	1.966(21)	2.746(28)	−0.3859(15)	0.59(22)
200	Obs.	1.164(10)	1.929(11)	2.682(11)		
	Calc.	1.156(7)	1.935(14)	2.703(17)	−0.3794(9)	0.62(15)

Figure 3 displays data taken at low energies with improved energy resolution. There is an additional line denoted by $Te_{0.95\ J}$ which can be attributed to the lowest tetramer ground-state transition.[11] Moreover, the lowest dimer transition (D_{2J}) exhibits a highly asymmetric shape. Obviously, the single-ion anisotropy splits the excited triplet state $|S=1\rangle$ into a doublet state $|M=\pm 1\rangle$ and a singlet state $|M=0\rangle$. The corresponding transition matrix elements have the approximate ratio of 2:1. A Gaussian least-squares fit results in a doublet-singlet separation of 0.07(1) meV, which can be rationalized by an anisotropy parameter $D=9(2)$ μeV according to Eq. (6). Figure 4 confirms this interpretation through the Q dependence of the intensities which nicely follow the predictions of cross-section formulas (7b) and (7c).

We analyzed the observed dimer transitions according to Eq. (4) which directly yields the temperature dependence of the bilinear and biquadratic exchange parameters J and K_D, respectively. The results are listed in Table I and shown in Fig. 5 as a function of the temperature-induced increase in the intradimer distance $R(T)$ with respect to R (20 K).[18] The bilinear exchange parameter J follows a linear relationship with $dJ/dR=1.63(14)$ meV/Å, whereas the biquadratic exchange parameter essentially remains constant at the average value $K=0.79(14)$ μeV.

V. MAGNETOELASTIC EFFECTS

A. Dimers

The total energy of an isolated pair of magnetic ions corresponds to the sum of the elastic energy W_{el} and the magnetic energy W_{ex} due to the exchange coupling J. The elastic energy density for cubic symmetry reads

$$u_{el}=\tfrac{1}{2}c_{11}(e_{xx}^2+e_{yy}^2+e_{zz}^2)+\tfrac{1}{2}c_{44}(e_{yz}^2+e_{zx}^2+e_{xy}^2)+c_{12}(e_{yy}e_{zz}+e_{zz}e_{xx}+e_{xx}e_{yy}), \quad (10)$$

where the c_{ik} and $e_{\alpha\beta}$ denote the elastic constants and strain components, respectively. The exchange coupling gives rise to a small deformation (contraction or dilatation) along the dimer bond axis, so that the local symmetry changes from cubic to tetragonal. For a tetragonal deformation (along the z axis), we have $e_{yz}=e_{zx}=e_{xy}=0$. Furthermore, assuming that the tetragonal deformation does not result in a volume change, we have $-e_{xx}=-e_{yy}=\frac{1}{2}e_{zz}=\frac{1}{2}(\frac{R-R_0}{R_0})$, where R_0 is the intradimer distance in the absence of the exchange interaction. Equation (10) then reduces to

$$u_{el}=\frac{3}{4}(c_{11}-c_{12})\left(\frac{R-R_0}{R_0}\right)^2. \quad (11)$$

The total energy of a dimer is then given by

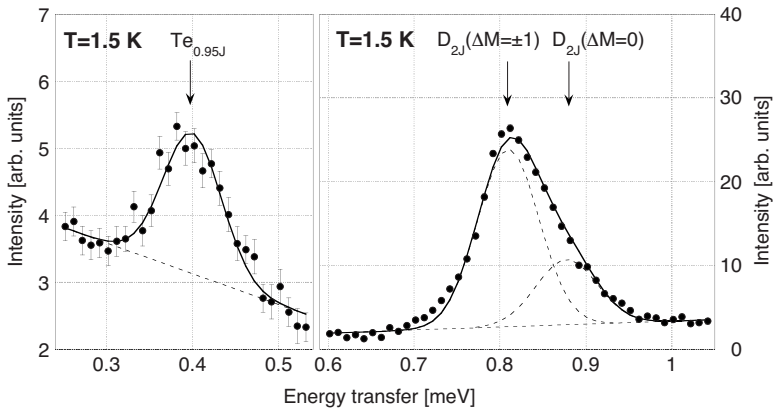

FIG. 3. Energy spectra of neutrons scattered from $KMn_{0.1}Zn_{0.9}F_3$ at $T=1.5$ K. The incoming neutron energy was 2.27 meV. The arrows and lines are as in Fig. 2.

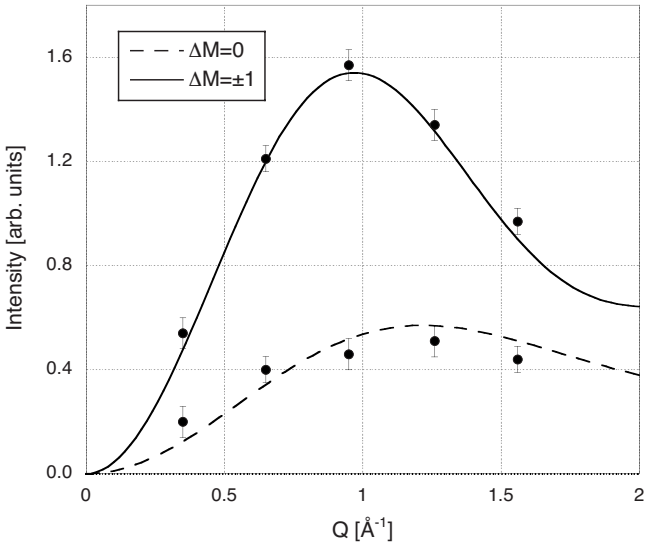

FIG. 4. Q dependence of the neutron cross section for the $\Delta M=0$ and $\Delta M=\pm 1$ components of the D_{2J} dimer transition of $KMn_{0.1}Zn_{0.9}F_3$. The circles denote the intensities observed at $T=1.5$ K. The dashed and full lines correspond to cross sections (7b) and (7c), respectively.

$$W_D = \frac{3}{4}v(c_{11}-c_{12})\left(\frac{R-R_0}{R_0}\right)^2 - 2J(R)\mathbf{S}_1\cdot\mathbf{S}_2$$
$$\approx \frac{3}{4}v(c_{11}-c_{12})\left(\frac{R-R_0}{R_0}\right)^2$$
$$-2\left[J(R_0)+\left(\frac{dJ}{dR}\right)_{R_0}(R-R_0)\right]\mathbf{S}_1\cdot\mathbf{S}_2, \qquad (12)$$

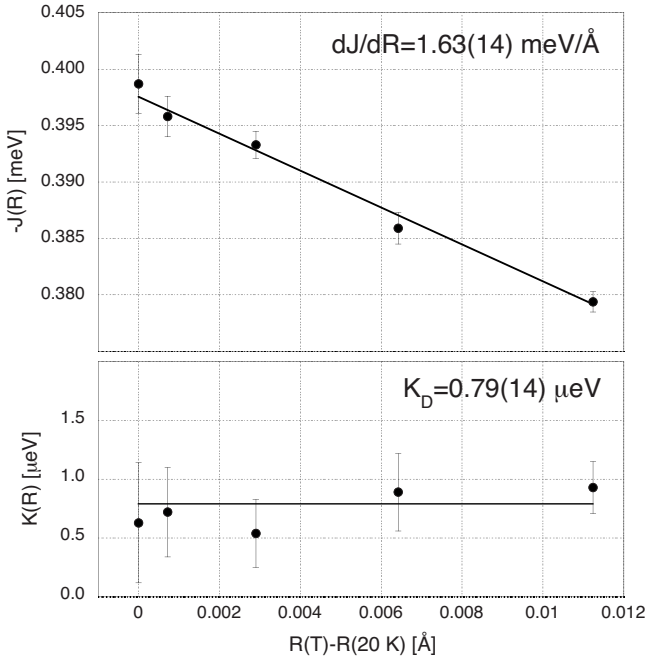

FIG. 5. Dependences of the bilinear and biquadratic exchange parameters J and K_D (listed in Table I) on the variation of the intradimer distance R with temperature. The lines are the results of a linear least-squares fit.

where $J(R)$ is expanded up to the first order. Here, v is the volume element occupied by the dimer. The distance R corresponding to the minimal total energy is obtained from $dW_D/dR=0$, resulting in

$$R-R_0 = \frac{4R_0^2}{3v(c_{11}-c_{12})}\left(\frac{dJ}{dR}\right)_{R_0}\mathbf{S}_1\cdot\mathbf{S}_2. \qquad (13)$$

Substituting $R-R_0$ back to Eq. (12) yields

$$W_D = -2J(R_0)\mathbf{S}_1\cdot\mathbf{S}_2 - \frac{4R_0^2}{3v(c_{11}-c_{12})}\left(\frac{dJ}{dR}\right)^2_{R_0}(\mathbf{S}_1\cdot\mathbf{S}_2)^2. \qquad (14)$$

By setting $v=2R_0^3$ and $R_0=a$ and comparing Eqs. (3) and (14), we can express the biquadratic exchange parameter K_D in terms of lattice, elastic, and magnetic properties,

$$K_D = \frac{2}{3a(c_{11}-c_{12})}\left(\frac{dJ}{dR}\right)^2. \qquad (15)$$

For $KMn_{0.1}Zn_{0.9}F_3$, the parameters c_{ik} are not known; thus, we interpolate between the values published for $KZnF_3$ and $KMnF_3$. With $c_{11}=133$ GPa, $c_{12}=51$ GPa (Ref. 19 and references therein), $a=4.0719(2)$ Å, and $\frac{dJ}{dR}=1.63(14)$ meV/Å from Fig. 5, we find $K_D=0.85(13)$ μeV which is in excellent agreement with $K_D=0.79(14)$ μeV determined from the present analysis of the dimer excitations. We therefore conclude that the presence of biquadratic exchange in $KMn_{0.1}Zn_{0.9}F_3$ is likely to be caused by the mechanism of exchange striction.

In the evaluation of the elastic energy density for tetragonal symmetry, we made the assumption of zero volume change which, however, is not a crucial condition. If we consider only a local, longitudinal distortion e_{zz} of the unit cell, i.e., setting $e_{xx}=e_{yy}=0$, the elastic energy density is simplified to

$$u_{el} = \frac{1}{2}c_{11}\left(\frac{R-R_0}{R_0}\right)^2. \qquad (16)$$

The minimization procedure as outlined above then yields

$$K_D = \frac{1}{ac_{11}}\left(\frac{dJ}{dR}\right)^2. \qquad (17)$$

By inserting the parameters for $KMn_{0.1}Zn_{0.9}F_3$, we find $K_D=0.78(13)$ μeV, which is in good agreement with K_D determined from Eq. (15).

B. Trimers

In close analogy to the procedure outlined in Sec. V A, the total energy of a trimer is given by

$$W_T \approx \frac{3}{4}v(c_{11}-c_{12})\left(\frac{R-R_0}{R_0}\right)^2$$
$$-2\left[J(R_0)+\left(\frac{dJ}{dR}\right)_{R_0}(R-R_0)\right](\mathbf{S}_1\cdot\mathbf{S}_2+\mathbf{S}_2\cdot\mathbf{S}_3). \qquad (18)$$

By setting $v=3R_0^3$, we find

$$W_T = -2J(R_0)(\mathbf{S}_1 \cdot \mathbf{S}_2 + \mathbf{S}_2 \cdot \mathbf{S}_3) - \frac{4}{9a(c_{11}-c_{12})}\left(\frac{dJ}{dR}\right)^2_{R_0}(\mathbf{S}_1 \cdot \mathbf{S}_2 + \mathbf{S}_2 \cdot \mathbf{S}_3)^2. \quad (19)$$

A comparison of Eqs. (5), (15), and (19) yields

$$K_T = L = \frac{4}{9a(c_{11}-c_{12})}\left(\frac{dJ}{dR}\right)^2 = \frac{2}{3}K_D. \quad (20)$$

We calculated the energies of the trimer transitions from the parameters J and K_D obtained from the dimer transitions and using relation (20) for K_T and L. The results are listed in Table II. Within experimental error, there is good agreement between the observed and calculated trimer energies, which means that the size of the next-nearest-neighbor exchange parameter is typically $|J'| < 1-2$ μeV. Furthermore, the good agreement reinforces our conclusion for K_D that exchange striction is also likely the origin of the biquadratic two-spin and three-spin exchange terms of Hamiltonian (5).

VI. CONCLUDING REMARKS

By analyzing the inelastic neutron scattering data observed for $KMn_{0.1}Zn_{0.9}F_3$, we were able to determine the temperature dependence of the exchange coupling of Mn^{2+} dimers, resulting in precise values of the bilinear and biquadratic exchange parameters J and K_D, respectively. We like to mention that biquadratic exchange terms cannot be directly derived from measurements of the spin-wave dispersion, since the bilinear and biquadratic coupling parameters J and K_D are combined as a joint prefactor of the wave-vector dependence.[20] Our value of $J=-0.399(3)$ meV at $T=20$ K is in good agreement with $J=-0.414(17)$ meV and $J=-0.405(8)$ meV derived for Mn^{2+} dimers and trimers, respectively, from neutron scattering investigations performed for a single crystal of $KMn_{0.1}Zn_{0.9}F_3$ at $T=4.3$ K (Ref. 21) as well as with $J=-0.43(3)$ meV derived from EPR experiments of Mn^{2+} doped $KZnF_3$ at $T=4.2$ K.[12] The analysis of the spin-wave dispersion measured for $KMnF_3$ at $T=4.2$ K gave $J=-0.328(4)$ meV and $J'=-9(2)$ μeV.[22] The much lower size of J is attributable to the different lattice constants, but the large size of J' is incompatible with the trimer energies determined in the present work. In the present work, the anisotropy parameter $D=9(2)$ μeV determined has about half the size of $|D|=17$ μeV derived from EPR measurements.[12]

Our results are in remarkable qualitative agreement with a recent study performed for Mn^{2+} pairs in the one-dimensional paramagnetic compound $CsMn_{0.28}Mg_{0.72}Br_3$.[6] More specifically, the results gave evidence for a strongly temperature- and pressure-dependent bilinear exchange parameter J and a nearly temperature- and pressure-independent biquadratic exchange parameter K_D, which could be rationalized to a large extent in terms of exchange striction. Moreover, a detailed study of Mn^{2+} trimers in $CsMn_{0.28}Mg_{0.72}Br_3$ resulted in explicit values for the two- and three-spin biquadratic exchange parameters, namely, $K_T=8.4(9)$ μeV and $L=6.1(6)$ μeV, respectively.[3] Within experimental error, K_T and L are roughly equal as predicted by Eq. (20) which adds further weight to support the exchange striction scenario. The results of the present work carried out for a three-dimensional paramagnet allow us now to generalize the statement that exchange striction is presumably the dominating mechanism for the presence of biquadratic exchange terms in the spin Hamiltonian of any magnetic insulator.

ACKNOWLEDGMENTS

This work was performed at the Swiss Spallation Neutron Source SINQ, Paul Scherrer Institut (PSI), Villigen, Switzerland. Financial support by the Swiss National Science Foundation is gratefully acknowledged.

[1] C. Herring, in *Magnetism*, edited by G. T. Rado and H. Suhl (Academic, New York, 1966), Vol. IIB, p. 1.
[2] R. Coldea, S. M. Hayden, G. Aeppli, T. G. Perring, C. D. Frost, T. E. Mason, S.-W. Cheong, and Z. Fisk, Phys. Rev. Lett. **86**, 5377 (2001).
[3] U. Falk, A. Furrer, H. U. Güdel, and J. K. Kjems, Phys. Rev. Lett. **56**, 1956 (1986).
[4] H. U. Güdel, U. Hauser, and A. Furrer, Inorg. Chem. **18**, 2730 (1979).
[5] E. A. Harris, J. Phys. C **5**, 338 (1972).
[6] Th. Strässle, F. Juranyi, M. Schneider, S. Janssen, A. Furrer, K. W. Krämer, and H. U. Güdel, Phys. Rev. Lett. **92**, 257202 (2004).
[7] P. W. Anderson, in *Magnetism*, edited by G. T. Rado and H. Suhl (Academic, New York, 1963), Vol. I, p. 25.
[8] C. Kittel, Phys. Rev. **120**, 335 (1960).
[9] E. N. Maslen, N. Spadaccini, T. Ito, F. Marumo, K. Tanaka, and Y. Satow, Acta Crystallogr., Sect. B: Struct. Sci. **49**, 632 (1993).
[10] O. Beckman and K. Knox, Phys. Rev. **121**, 376 (1961).
[11] U. Falk, A. Furrer, N. Furer, H. U. Güdel, and J. K. Kjems, Phys. Rev. B **35**, 4893 (1987).
[12] J. J. Krebs, J. Appl. Phys. **40**, 1137 (1969).
[13] A. Stebler, H. U. Güdel, A. Furrer, and J. K. Kjems, Inorg. Chem. **21**, 380 (1982).
[14] A. Furrer and H. U. Güdel, J. Magn. Magn. Mater. **14**, 256 (1979).
[15] A. Podlesnyak, V. Pomjakushin, E. Pomjakushina, K. Conder, and A. Furrer, Phys. Rev. B **76**, 064420 (2007).
[16] S. Kirkpatrick, Rev. Mod. Phys. **45**, 574 (1973).
[17] W. J. L. Buyers, T. M. Holden, E. C. Svensson, and D. J. Lockwood, Phys. Rev. B **30**, 6521 (1984).
[18] F. Rodriguez and M. Moreno, J. Phys. C **19**, L513 (1986).
[19] R. R. Becher, M. J. L. Sangster, and D. Strauch, J. Phys.: Condens. Matter **1**, 7801 (1989).
[20] U. Falk, A. Furrer, J. K. Kjems, and H. U. Güdel, Phys. Rev. Lett. **52**, 1336 (1984).
[21] E. C. Svensson, M. Harvey, W. J. L. Buyers, and T. M. Holden, J. Appl. Phys. **49**, 2150 (1978).
[22] S. J. Pickart, M. F. Collins, and C. G. Windsor, J. Appl. Phys. **37**, 1054 (1966).